

We are IntechOpen, the world's leading publisher of Open Access books Built by scientists, for scientists

4,800

Open access books available

122,000

International authors and editors

135M

Downloads

Our authors are among the

154

Countries delivered to

TOP 1%

most cited scientists

12.2%

Contributors from top 500 universities



WEB OF SCIENCE™

Selection of our books indexed in the Book Citation Index
in Web of Science™ Core Collection (BKCI)

Interested in publishing with us?
Contact book.department@intechopen.com

Numbers displayed above are based on latest data collected.
For more information visit www.intechopen.com



Magnetron Sputtered BG Thin Films: An Alternative Biofunctionalization Approach – Peculiarities of Bioglass Sputtering and Bioactivity Behaviour

George E. Stan¹ and José M.F. Ferreira²

¹*Nanoscale Condensed Matter Physics Department,
National Institute of Materials Physics, Bucharest-Magurele*

²*Department of Ceramics and Glass Engineering, CICECO, University of Aveiro, Aveiro*

¹*Romania*

²*Portugal*

1. Introduction

Nowadays orthopaedic and dental metallic prostheses are widely used in the medical field, the most common being 316L stainless steel, Co-Cr alloys, titanium (Ti) or Ti superalloys. These metallic materials were preferred due to their good mechanical performance, adequate stiffness, non-magnetic properties and to their intrinsic property of promoting on their surface in contact with air or biological media a very thin and biologically inert oxide film (Cr_2O_3 in case of stainless steel and Co-Cr alloy or TiO_2 for (Ti) and Ti alloys), which could act as a metallic ions diffusion barrier layer. However, due to corrosion in the aggressive biological media, this thin protective layer could easily be shattered locally and metallic ions could enter the biological environment causing adverse reactions. Allergies, bone necrosis and the accumulation of metal particles in organs were detected in some cases (C. Brown et al., 2006; C. Brown et al., 2007).

The new generation of orthopaedic and dental implants aims towards the increase of biocompatibility by replacing the biotolerated metallic surfaces with bioactive ones. For increasing the bioactivity of prostheses and implants, there were designed devices coated with biologically active materials such as hydroxyapatite, simple or doped with different metallic ions or functional groups, various calcium phosphates, and more recently, bioglasses and glass-ceramics. Therefore, considerable attention has been given to the use of implants with bioactive fixation in the past decade (L.L. Hench & J. Wilson, 2003).

The commercial solution currently applied worldwide is the orthopaedic and dental titanium implants biofunctionalized with thick ($>50 \mu\text{m}$) bioactive coatings of hydroxyapatite [HA , $\text{Ca}_{10}(\text{PO}_4)_6(\text{OH})_2$] prepared by plasma spraying.

Although this type of implant structure proved to be successful clinically, there are still significant deficiencies hard to ignore (e.g. low mechanical strength, difficulty in controlling

the solubility *in vivo*, etc.), both in the preparation of biofunctional coatings and in their long-term *in situ* functional operation (Batchelor & Chandrasekaran, 2004; Epinette et al., 2003). Albeit their biological properties are excellent, the large thickness of the HA films synthesized by plasma spray determines the susceptibility to cracking and/or delamination due to poor adherence, phenomena that will allow the diffusion of implant's metal ions into the surrounding tissues and can lead to malfunctioning of the medical device in question. To address these shortcomings, currently a variety of alternative coating methods are being studied, from wet sol-gel technology, electrophoretic deposition and pulsed laser ablation, to magnetron sputtering for producing thinner adherent films of hydroxyapatite, calcium phosphates or bioactive glasses.

Bioactive glasses or bioglasses (BG) are osteoproducer-type inorganic materials far from proving their fully operative potential yet. Since the discovery of Bioglass® (45S5) by Larry Hench (L.L. Hench & J. Wilson, 2003), many bioglass compositional systems have been proposed and proved their suitability to form a bond with the living bone tissue and enhance the osteosynthesis at the implant site due to the favourable chemical interactions with the body fluid in the tissue rehabilitation process.

The behaviour of bioactive glasses in the formation of new bone tissue depends on the chemical composition and textural properties (Saravanapavan & Hench, 2001; Sepulveda et al., 2002). Glasses of the $\text{Na}_2\text{O}-\text{CaO}-\text{P}_2\text{O}_5-\text{SiO}_2$ system can be either formed from the traditional melt-quenching (Wu et al., 2011) or by the modern sol-gel method (Balamurugan et al., 2007). It has also been proved that an increase in the growth rate of apatite-like layer as well as the wider bioactivity were observed depending on the compositional range used for the preparation of bioglass (Rámila & Vallet-Regí, 2001; Vallet-Regí et al., 2003). The recent progresses made on the synthesis and processing of bioglasses that allowed the formulation of new compositional systems with lower thermal expansion coefficients (CTE) and enhanced bioactivity (Agathopoulos et al., 2006; Balamurugan et al., 2007; Tulyaganov et al., 2011) reopened the issue of bioglass coatings as a viable implantologic solution for load-bearing applications.

Generally bioactive glasses and glass-ceramics have been extensively developed and investigated for non-loading applications as bone grafts, fillers or auricular implants owing to their ability to form a bond with the living bone and put into clinical use following many years of animal testing in a variety of experimental models (Hench, 1991; Ratner et al., 2004).

To the best of our knowledge there are still no commercial titanium (Ti) implants functionalized with bioactive glass (BG) coatings, due to their poor adhesion to the metallic substrate determined by their native friability and to the significant mismatch of the CTEs for the BG coating ($12-17 \times 10^{-6}/^\circ\text{C}$) and Ti-based substrate ($\sim 9.2-9.6 \times 10^{-6}/^\circ\text{C}$). Pull-out adherence values higher than 40 MPa are accepted for such implant-type coatings (ASTM, 2009; FDA, 1997; ISO/DIS, 1999).

The research on implants with thick coatings made of bioglasses prepared by using an enamelling process has shown that, in time, cracks appear in the coatings, allowing metallic ions to spread inside the human body, and producing finally their delamination. Moreover, in comparison with hydroxyapatite films, the control of composition and adhesion to metallic substrates seems to be more difficult to accomplish in the case of the BG ones.

The implants must simultaneously satisfy requirements such as biocompatibility, strength, corrosion resistance and sometimes aesthetics. It is widely accepted that both mechanical properties and chemical composition are important factors in the preliminary physiological bond of such implants to living tissues. Low mechanical properties are the major problem that prevented the use of BG/Ti structures for load-bearing applications.

This chapter aims to introduce magnetron sputtering technique as a solid alternative for bioactive implants' functionalization, taking a new step in the research of implant-type structures based on bioactive glasses. The chapter will present our recent findings on the correlation between bioactive powder targets/RF-MS deposition parameters versus composition tailoring of BG thin films, and their mechanical and in vitro behaviour in simulated body fluids (SBF). Understanding these correlations could be important for fundamental physics, materials science and prosthetic medicine as well as from a technological point of view.

Radio Frequency - Magnetron Sputtering (RF-MS) deposition is nowadays one of the most popular techniques to grow thin films in research and in decorative and semiconductor industry. In this method the plasma is used as a source of energetic ions (within the energy range 10–500 eV) that are accelerated towards the cathode target. When energetic ions reach the target surface with energy above the surface binding energy (the minimum threshold is typically somewhere in the range 10–100 eV), an atom can be ejected. This way free atoms and clusters are produced by sputtering, which are subsequently deposited on a substrate as well as the reactor chamber walls (Palmero et al., 2007).

Recently, Radio Frequency - Magnetron Sputtering (RF-MS) has emerged a promising alternative for preparing adherent bioactive glass films (G.E. Stan et al., 2009; G.E. Stan et al., 2010a, 2010b, 2010c, 2010d) due to its tailoring possibilities and due to some advantages: low pressure operation, low substrate temperature, high purity of the films, ease of automation, and excellent uniformity on large area substrates (Wasa et al., 2004).

In this chapter we present recent findings on the adherence and bioactivity of bioglass coatings prepared by magnetron sputtering technique. The study will indicate how features such as composition, structure, adherence and bioactivity of bioglass films can be tailored simply by altering the magnetron sputtering working conditions, proving that this less explored technique is a promising alternative for preparing implant-type coatings. Extensive multi-parametrical structural, compositional, morphological and mechanical characterizations were employed by FTIR, GIXRD, SEM, and pull-out tests.

2. Solutions for increasing the adherence at the titanium substrate / glass coating interface

It is widely accepted that the integrity of the substrate/coating interface is always critical in determining the performance and the reliability of any implant-type coating. Generally, low values of adhesion for bioglass coatings were published (Mardare et al., 2003; Goller, 2004; Peddi et al., 2008). Among the deposition techniques available for producing bioglass coatings, magnetron sputtering is the less explored. Only three papers have been published by other groups on this topic to the best of our knowledge (Mardare et al., 2003; Wolke et al., 2008; Saino et al., 2010). The main impediment in using bioglass coatings as implant

applications is the high thermal expansion coefficients of bioglass, about $12\text{--}17 \times 10^{-6}/^{\circ}\text{C}$, relative to that of medical-grade titanium $\sim 9.2 \times 10^{-6}/^{\circ}\text{C}$ (L.L. Hench & J. Wilson, 2003; Goller, 2004).

The adherence of the substrate/coating interface is always considered when estimating the implant-type coating reliability in medical practice. The mechanical quality of the interface can be evaluated by pull-out strength measurements. The pull-out measurements were carried out using an adhesion tester – DFD Instruments PAT MICRO adhesion tester AT101 (maximum pull force = 1 kN) equipped with Φ 2.8 mm stainless steel test elements. The test elements were glued to the film's surface with a cyanoacrylate one-component Epoxy adhesive, E1100S. The stub surface was first polished, ultrasonically degreased in acetone and ethanol and dried in a nitrogen flow. After gluing, the samples were placed in an oven for thermal curing ($130^{\circ}\text{C}/1$ h). Each test element was pulled-out vertically with a calibrated hydraulic pump until detachment. The experimental procedure was conducted in accordance with the ASTM D4541 and ISO 4624 standards. The adhesion strength was determined from the recorded failure value divided by the quantified detached surface area. Mean values and standard deviations were computed. The statistical significance was determined using an unpaired Student's t-test. The differences were considered significant when $p < 0.05$.

In a first step, a bioglass (BG1) mild-pressed powder having the following composition (wt %): SiO_2 - 55, CaO - 15, P_2O_5 - 10, K_2O - 10, MgO - 5, Na_2O - 5, having a low CTE ($\sim 10.2 \times 10^{-6}/^{\circ}\text{C}$) was used as cathode target. The BG1 samples preparation details are presented in Table 1.

Bioglass target	Sputtering pressure (Pa)	Working atmosphere	Substrate type	Film thickness	Post-dep. heat-treatments
BG1	0.3	Ar	Ti6Al7Nb	750 nm	$550^{\circ}\text{C}/2\text{h}$ in air $750^{\circ}\text{C}/2\text{h}$ in air

Table 1. BG1 sputtering deposition conditions and additional sample preparation details

The as-deposited structures as well as the heat-treated ones were investigated. Figure 1 presents the GIXRD patterns of the BG1 structures before and after the devitrification heat-treatments. The structure of the as-deposited film is amorphous at the sensitivity limit of the measurement. The amorphous component is probably based on amorphous silica, as it can be deduced from the main hump centred on $2\theta \approx 22^{\circ}$. After heat treatment at 550°C , several weak TiO_2 -rutile – ICDD: 12-1276 lines appear, whose intensity increases by annealing at 750°C . During heat treatment at 750°C , crystallization occurs in the layer, but the amorphous component only slightly diminishes. The few rather intensive peaks which appear, were assigned to: $\text{Na}_2\text{Mg}(\text{PO}_3)_4$ – ICDD: 22-477 and TiO_2 -rutile. There are also several weak lines that might be associated with small percents of perovskite (CaTiO_3 – ICDD: 78-1013) and oxygen deficient titanium oxides (Ti_2O – ICDD: 11-0218 and TiO – ICDD: 72-0020). The formation of calcium titanate and, at least partly, of titanium oxides in the heat-treated samples, is due to the inter-diffusion at the film-substrate interface. The presence of perovskite in heat-treated hydroxyapatite films deposited onto titanium had already been observed by other authors (Wei et al., 2005; Berezhnaya et al., 2008).

In case of the as-deposited and 550°C annealed structures the failure always occurs in glue's volume without damaging the film integrity at an average value of 85 MPa. This represents the bonding limit of the resin, as confirmed by the manufacturer. For the structures annealed at 750°C the adherence was estimated at 72.9±7.1 MPa, the film being detached each time. However, the measured film-substrate adhesion values are much higher than those reported in literature (Mardare et al., 2003; Goller, 2004; Peddi et al., 2008).

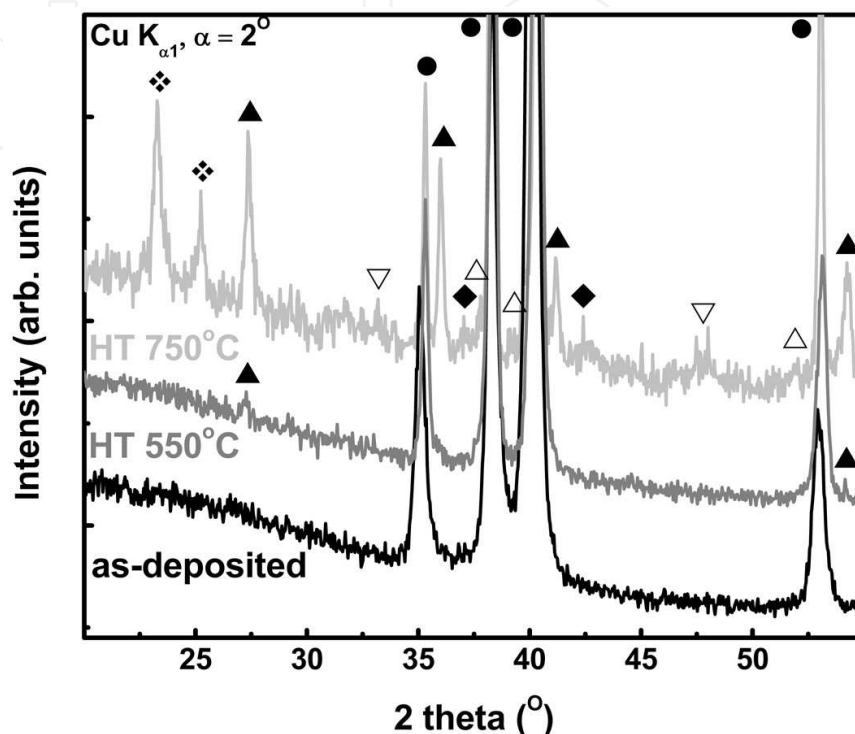


Fig. 1. GIXRD patterns collected for the BG1 films before and after the post-deposition heat-treatments: ● - titanium alloy substrate; ❖ - Na₂Mg(PO₃)₄; ◆ - CaTiO₃; ▲ - TiO₂-rutile; △ - Ti₂O; ▽ - TiO

These high values of pull-out strength for the as-deposited coatings, and those annealed at 550°C, are attributed to the sputter cleaning and ion bombarding processes of the substrate, done before deposition (G.E. Stan et al., 2009). As it is known, the poor adhesion of the coatings could be ascribed to the natural oxide layers present on the titanium alloy surface prior deposition. An optimal solution for removing these contaminants in order to increase the adherence is an argon plasma etching pre-treatment of the titanium substrates. The sputter cleaning process largely removes not only the native oxide layers, but also the adsorbed gas molecules, to produce a clean, highly active surface (Lacefield, 1988). The argon ion bombarding process during sputtering might enhance the atomic diffusion and mixing in the near-interface region. The etching process has been optimized by tuning plasma power (~200 W), surface DC bias (0.4 kV) and etching time (10 min), based on own experience and literature (Mattox, 1994). The sputtering time offers a maximum of the adhesion properties after 10 min, as a result of the removal of surface oxides and contaminants, which leads to good bonding at the coating-substrate interface (G.E. Stan et al., 2009).

The decrease of the adherence after heat-treatment at 750°C, is due the BG layers/titanium substrate dilatation coefficients misfit at high temperatures and to the strong oxidation

phenomena which led to the formation of needle-shaped rutile crystals agglomerates which penetrate through the film (Fig. 2).

On the other hand, the formation during the heat-treatments of a perovskite-type phase (CaTiO_3) suggested an inter-diffusion phenomenon between the coating and the substrate during heat-treatment, which appears to be the predominant factor in determining a film adhesion even in case of high temperature annealing treatments. The formation of various types of titanium oxides and sub-oxides is also in agreement with this hypothesis. This finding could be further exploited by designing special heat-treatments which would lead to nucleation at the interface of inter-mix BG-Ti phases with role in strengthening the coating adherence.

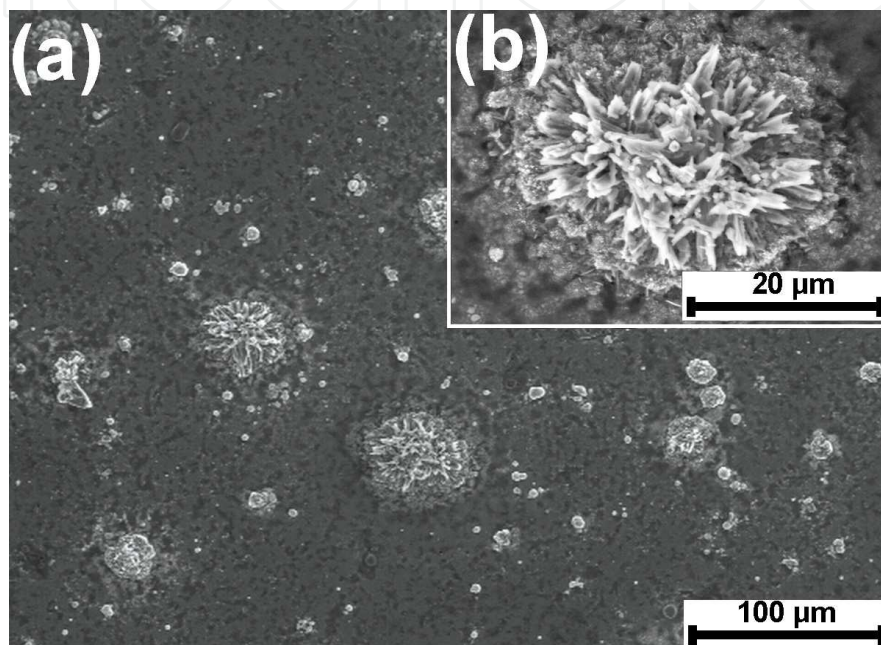


Fig. 2. SEM images of a BG1 film heat-treated in air at 750°C/2h

The classical 45S5 composition system (SiO_2 – 45 wt%, CaO – 24.5 wt%, P_2O_5 – 6 wt%, Na_2O – 24.5 wt%), patented by Hench a couple of decades ago, has a significantly higher thermal expansion coefficient ($15 - 17 \times 10^{-6}/^\circ\text{C}$) than the titanium and titanium alloys materials. 45S5 commercial powders have been mild-pressed to prepared cathode targets (BG2). The BG2 samples preparation details are presented in Table 2.

Bioglass target	Sample type	Sputtering pressure	Working atmosphere	Substrate type	Film thickness	Post-dep. heat-treatments
BG2	Simple BG2-A (BG/Ti)	0.3 Pa	Ar	cp-Ti grade 4	~ 700 nm	650°C/2h in air
BG2	Graded BG2-G (BG/BG _{1-x} Ti _x /Ti)	0.3 Pa	Ar	cp-Ti grade 4	~ 770 nm	650°C/2h in air

Table 2. BG2 sputtering deposition conditions and additional sample preparation details

In such a case, in the attempt to increase the adherence properties of the BG2 film to the titanium substrate, a buffer layer with chemical gradient of composition was introduced. The graded $BG_{1-x}Ti_x/Ti$ ($x=0-1$) structure was prepared by a slow continuous shifting of the rotating substrate holder during the co-sputtering deposition, from the Ti target towards the BG one (G.E. Stan et al., 2010c). This way, a functionally graded transition zone with a variable chemical composition was forming between the BG biofunctional coating and the Ti substrate (Fig. 3). This process lasted for 5 minutes, the graded layer thickness being estimated at ~ 70 nm. Next, the formed graded structure was placed in front of the BG target and the sputtering continued for 1 hour in order to deposit the functional BG layer with a thickness of ~ 700 nm (BG2-G).

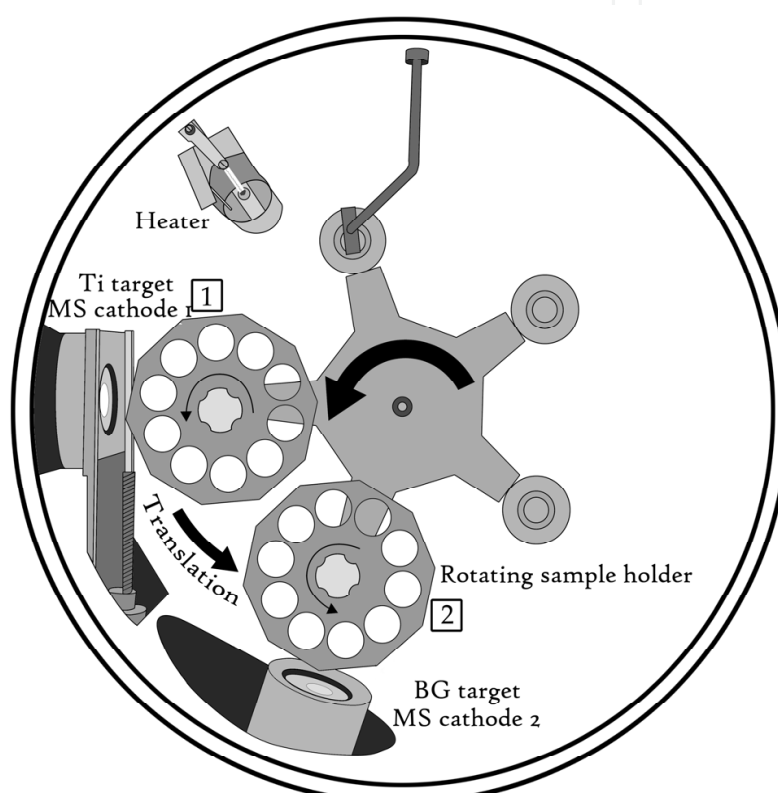


Fig. 3. Schematic diagram of the graded $BG_{1-x}Ti_x/Ti$ ($x=0-1$) structure deposition by magnetron co-sputtering

For bonding strength comparison, we synthesized by RF-MS, under identical experimental conditions, 700 nm BG/Ti “abrupt coatings” (BG2-A) without the intermediate buffer layer between the substrate and the film.

As an improvement of the mechanical and biological properties of films is known to be achieved by the transformation of BG into glass-ceramics via heat-treatments (Peitl Filho et al., 1996; El Batal et al., 2003), we have chosen for our study an annealing temperature of $650^{\circ}C/2h$ in order to induce the partial crystallization of the combeite ($Na_2CaSi_2O_6$) phase. As known (Lefebvre et al., 2007), the crystallization of the combeite is reached within the range ($610 - 700^{\circ}C$) and the larger the temperature, the higher the crystallization degree. Low heating and cooling rates ($1^{\circ}C/min$) have been applied in order to minimize the residual mechanical stress in films at the end of the thermal cycle (Berbecaru et al., 2010).

The GIXRD analysis of the BG2-G coating before heat treatment confirmed the amorphous nature of the deposited films (Fig. 4). The titanium sub-oxide phase, Ti_3O (ICDD: 73-1583) was present in the structure of the untreated sample. The structure was crystallized after heat-treatment with combeite - ICDD: 75-1687, $CaSiO_3$ (wollastonite) - ICDD: 42-550, and Na_3PO_4 - ICDD: 76-202 as main crystalline phases. There was noticed a strong signal originating from the Ti substrate - ICDD: 44-1294. After the heat-treatment, Ti lines were shifted towards lower angles, simultaneously with a strong broadening. Moreover, the Ti sub-oxide completely disappeared and was replaced by two well crystallized Ti dioxide phases, anatase - ICDD: 89-4203 and rutile - ICDD: 12-1276 (G.E. Stan et al., 2010c).

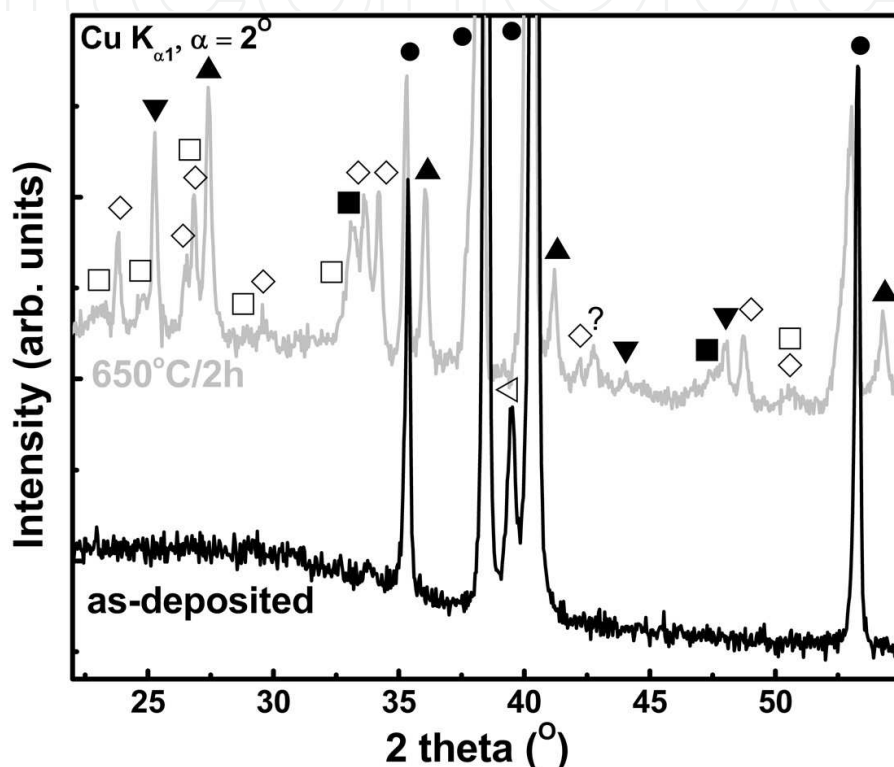


Fig. 4. GIXRD patterns collected for the BG2 films before and after the post-deposition heat-treatments: ●- titanium substrate; ◇- combeite ($Na_2CaSi_2O_6$); □- wollastonite ($CaSiO_3$); ■- Na_3PO_4 ; ▼- TiO_2 -anatase; ▲- TiO_2 -rutile; ◁- Ti_3O

The partial crystallization of the BG structure may prove advantageous for biomedical applications as it results in improved bioactivity due to formation on their surface of calcium phosphate (CaP) rich layers in contact with simulated body media, as would be demonstrated in the Subsection 3.3. The formation of such an apatite type layer is very important for bone growth and bonding ability.

A statistical analysis was performed based on the average value for ten different BG samples in case of each type of structure. For the BG2-A structure, the bonding failure occurred at a mean value of 29.2 ± 7 MPa (G.E. Stan et al., 2010c). This is a rather low bonding strength value, but similar to those reported in literature (Mardare et al., 2003; Goller, 2004; Peddi et al., 2008). This effect is mainly due to the significant difference between the thermal expansion coefficients of the BG film and the titanium substrate at high temperatures.

A 1.7 times higher bonding strength (50.3 ± 5.8 MPa) was obtained in case of the BG2-G structure (G.E. Stan et al., 2010c). The bonding strength to Ti substrates characteristic to heat-treated BG2-G samples is larger than current values reported in literature (50 MPa vs. 30 MPa). The BG2-G design eliminates the material interface discontinuity due to the formation of a BG_xTi_{1-x} ($x=0-1$) functionally graded buffer layer that improves the bonding strength. The result indicated that the synthesis of BG structures with graded buffer layers is a feasible solution for preparing adherent BG coatings, even in case of bioglasses with high thermal expansion coefficients (G.E. Stan et al., 2010c).

In the following paragraphs results will be presented depicting the influence of typical sputtering variables (deposition pressure, working gas composition) on the BG thin films adherence. For these studies a novel complex bioglass powder composition (BG3) was chosen as cathode target (wt %): SiO_2 - 40.08, CaO - 29.1, MgO - 8.96, P_2O_5 - 6.32, CaF_2 - 5.79, B_2O_3 - 5.16, and Na_2O - 4.59. The deposition conditions are presented in Table 3.

Bioglass target	Sample denomination	Sputtering pressure	Working atmosphere composition	Substrate type	Deposition time	Film thickness
BG3	BG3-1	0.2 Pa	100%Ar	cp-Ti grade 1	70 min	646 nm
BG3	BG3-2	0.3 Pa	100%Ar	cp-Ti grade 1	70 min	510 nm
BG3	BG3-3	0.4 Pa	100%Ar	cp-Ti grade 1	70 min	480 nm
BG3	BG3-4	0.3 Pa	93%Ar+7%O ₂	cp-Ti grade 1	70 min	380 nm

Table 3. BG3 sputtering deposition conditions and additional sample preparation details

The GIXRD measurements evidenced the amorphous state of all as-deposited BG3 thin films. Figure 5 displays the SEM micrographs of the as-deposited BG films. One can see important modifications of the morphology at a sub-micrometric level when varying the deposition conditions. The SEM micrographs revealed well-adhered films with a homogeneous surface microstructure for all the as-deposited samples. No signs of micro-cracks or delaminations were noticed. The rough microstructure, consisting in parallel alternant, stripe-like tall regions, delimited by narrow depressions was probably induced by titanium substrate, while the fine structure consists of nano-sized merged-granules (Fig. 5 - inset). One can not see significant influence of pressure upon the microstructure (BG3-1, BG3-2 and BG3-3). In case of reactive atmosphere (BG3-4) the films' surfaces presented interesting features. The coating is uniformly covered by tower-shaped nano-formations with an average diameter of ~ 70 nm. The tower-shaped nano-aggregates seem to be ingrowths nucleated on a matrix which is similar to BG3-1, BG3-2 and BG3-3 (G.E. Stan et al., 2011).

The physics of the magnetron sputtering process at different working pressures and compositions of the working atmosphere determines the thickness and morphology of the as-deposited BG films. The films' thicknesses varied between 380 and 646 nm, the thicker for the lowest pressure non-reactive deposition atmosphere. The decrease of the film thickness with the increase of Ar pressure from 0.2 to 0.4 Pa might be assigned to a decreased fraction

of sputtered particles reaching the substrate, due to the increased probability of collision with other particles when running from target to substrate. But, despite the masses of the sputtered atoms (M_s) in case of BG material are comparable to that of the background Ar gas ($M_{Ar}/M_s = 1-1.8$), thus favouring the kinetic energy loss by collision, the thermalization or removal while running towards the substrate is unlike because of the short target-to-substrate distance (only 30 mm) (Palmero et al., 2007, G.E. Stan et al., 2010d).

Under these deposition conditions it is highly probable that the main phenomenon leading to decreasing growth rate of BG films is the occurrence of charge transfer reactions in Ar (van Hattum et al., 2007). These processes lead to possible modifications of the energy and extent of the argon ion and neutral bombardment during the deposition in the considered pressure region. The occurrence of resonant charge transfer reactions is known to lower the energy of bombarding ions, determining significant variations of the sputter yield.

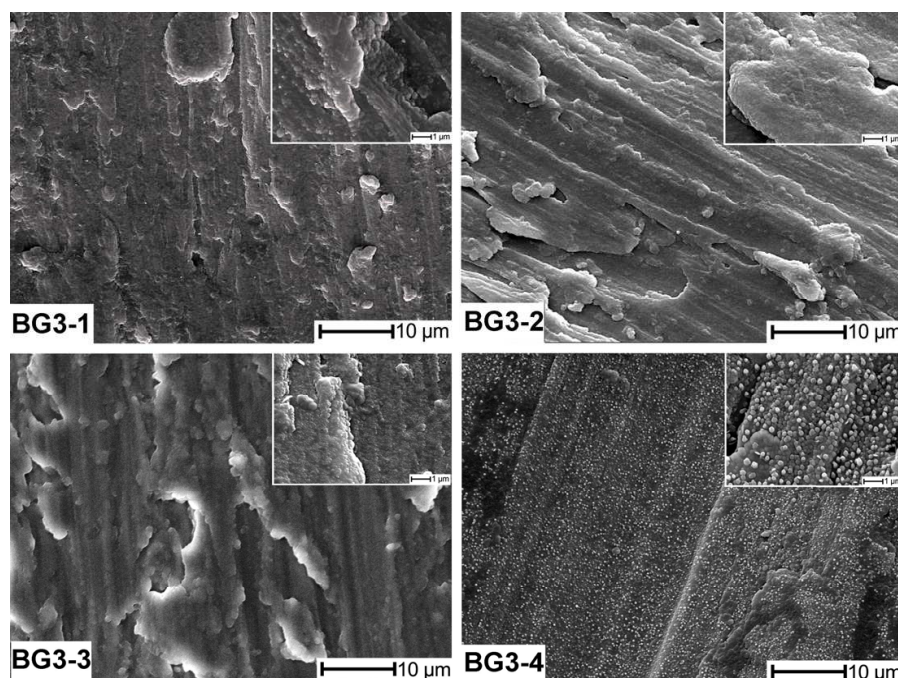


Fig. 5. SEM images of as-deposited BG3 sputtered films

The decreased deposition rate observed in the presence of oxygen in the working atmosphere can be attributed to “target poisoning” induced by chemisorption and oxygen ion implantation (Berg & Nyberg, 2005). During the sputtering process the BG target is bombarded by ions from the plasma, including reactive oxygen ions. This leads to the formation of a compound film not only on the substrate as desired, but also on the sputtering target. This results in a significantly reduced sputter yield, and thereby, a reduced deposition rate (G.E. Stan et al., 2010a).

Significant pull-out adherence differences were found function of sputtering deposition regime. In the case of BG3-1 and BG3-2 films, the failure occurred in the epoxy adhesive’s volume at 84.8 ± 1.5 MPa without damaging the film integrity (G.E. Stan et al., 2011). As this value represents the bonding limit of the epoxy adhesive as confirmed by the manufacturer, the true BG coating – Ti substrate bonding strength could be even higher. This adhesion value is much higher than the usual ones reported in literature (Mardare et al., 2003; Goller,

2004; Peddi et al., 2008). For the films deposited at higher argon pressure (BG3-3), the adherence dramatically decreased to a mean value of 34.2 ± 12.0 MPa, the bonding failure occurring at the film - substrate interface. When using a reactive atmosphere (BG3-4), but keeping the total pressure constant at 0.3 Pa, the adhesion strength of monolithic BG coating declined down to 44.0 ± 6.8 MPa (G.E. Stan et al., 2011). Similar adherence values have been generally reported in literature (Mardare et al., 2003; Goller, 2004; Peddi et al., 2008). The two tailed t-testing, assuming unequal variances, showed statistically significant differences between the results obtained for the different coatings ($p < 0.05$).

The excellent adherence value of BG3-1 and BG3-2 films must be emphasized. The adherence values are significantly higher than those reported in literature for this kind of implant coatings, thereby opening new perspectives in implantology. The high adherence is related to the processes characteristic of magnetron plasma sputtering. At a lower pressure the sputtered atoms collide with the substrate with higher kinetic energy, creating the possibility of forming chemical bonds with atoms from the substrate or being implanted into substrate. Such phenomena could lead to an increased adherence in case of the BG3-1 and BG3-2 films. Using a higher pressure (BG3-3) results in a spatial density variation of the background gas and affects the magnetron sputtering discharge as well as the transport of the particles towards the substrate. The energy flux at the substrate is thus affected, which in turn affects the properties of the growing film such as density, grain size, columnar structure, stoichiometry, coverage and adhesion (G.E. Stan et al., 2011). Moreover, their surface mobility is dramatically reduced, causing possible film inhomogeneities, such as voids or clustering hillocks (G.E. Stan et al., 2010d). In case of BG3-4 films, the presence of the tower shaped glassy nano-aggregates on the BG surface could be the underlying reason for the decreased adherence. Usually when dealing with tensile forces, rupture involves only a few molecules in the material causing the whole specimen to fracture in a “domino effect” (G.E. Stan et al., 2011).

3. Bioactivity tailoring of bioglass and glass-ceramic sputtered thin films

3.1 As-deposited films analysis

An implant-type ideal coating should constitute a proper mechanical support while exhibiting an enhanced bioactivity.

The bioglass structure is very complex; there is only short and medium range order determined by chemical bounding and steric hindrance. The silica-based glass structure is generally viewed as a matrix composed of SiO_4 tetrahedra connected at the corners to form a continuous tri-dimensional network with all bridging oxygen (BOs). The SiO_4 tetrahedra network is slightly distorted due to variations in the bond angles and the torsion angles. The network modifiers (alkali and alkali-earth ions typical to bioglasses) enter the structure as singly or double charged cations and occupy interstitial sites. Their charge is compensated by non-bridging oxygen bonds (NBOs), created by breaking bridges between adjacent SiO_4 tetrahedra. The increase of modifier content generates the creation of large NBOs concentrations, reducing the connectivity of the BG network, with direct effect upon electrical conduction, the thermal expansion coefficient, glass transition temperature, chemical corrosion in aqueous media and reactivity (Serra et al., 2002; Liste et al., 2004).

The biomineralization activity of a bioglass is influenced by the concentrations of bridging and non-bridging oxygen atoms per silicon oxygen tetrahedron as a function of the alkali oxide concentration. The Q^n notation expresses the concentration of bridging oxygen atoms per tetrahedron, where the value of n is equal to the number of bridging oxygen atoms (Elgayar et al., 2005). The Q^n species are detected in IR spectra in the 850–1200 cm^{-1} region by broad bands developing in accordance with the glass alkali and alkali-earth composition. The depolymerization of silicate network is defined by bands present at lower wave numbers in the absorption envelope.

RF-MS is known as a non-equilibrium preparation method which generally produces non-stoichiometric films relative to the sputtering target composition. Therefore it is possible to prepare nanostructured BG films with stoichiometries which can not be obtained by the classical equilibrium bulk synthesis methods. However, the preliminary studies have revealed that by varying the deposition pressure and/or working atmosphere composition it is possible to obtain a stoichiometric transfer even for complex compositional systems such as BGs (G.E. Stan et al., 2010a, 2010b, 2010c, 2010d). When selecting the RF-MS deposition parameters for the BG films preparation, one should take into account the standard free energy of the oxidation reactions of the different elements involved (Alcock, 2001):

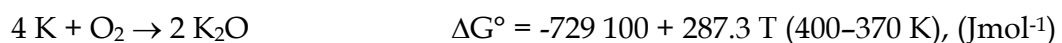
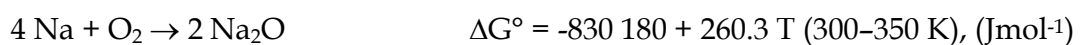
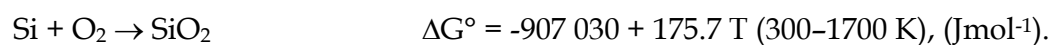
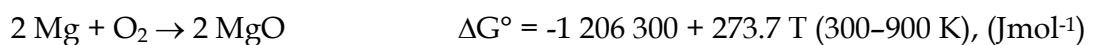
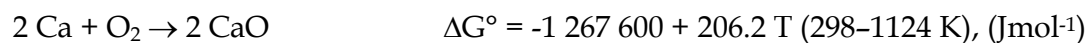


Table 4 presents the BG films atomic concentration with respect to the cathode target original composition. As can be seen Ca is among the most reactive elements towards oxygen, and this explains why its concentration decreased in the BG3 films. The reaction between Ca and the impinging oxygen ions might account for target poisoning by binding calcium ions at the target's surface. According to this reasoning, one would expect almost similar concentration changes for Mg since its standard free energy of oxidation is close to that of Ca. However, Table 4 shows that higher concentrations of Mg were determined for all the films in comparison to the starting bioglass powder. This suggests that the atomic weight might also play a role, with heavier elements diffusing more slowly. Na enjoys of these two characteristics, i.e., it is lighter and its standard free energy of oxidation is lower, being more easily sputtered. The formation of P_4O_{10} , and especially of PO requires higher partial pressure of oxygen. This might explain why a so small amount of P was found in the films. On the other hand, silicon also forms two possible phases, SiO_2 or SiO upon oxidation with the first being favored at the temperature of the experiments. The formation of these species also requires higher partial pressure of oxygen in comparison to the formation of oxides of Na, Ca, Mg (G.E. Stan et al., 2011).

Sample type	Concentration (at %)					
	Si	Ca	P	Na	Mg	K
BG1 powder target	50.28	14.68	7.73	8.85	6.81	11.65
BG1 as-deposited film	50	16	10	19	2.6	2.4
BG2 powder	36.34	21.2	4.1	38.36	-	-
BG2 as-deposited film	35	20	2	43	-	-
BG3 powder target	38.43	34.18	5.9	8.5	12.88	-
BG3-1 as-deposited film	30	27	3	20	20	-
BG3-2 as-deposited film	30	32	3	16	19	-
BG3-3 as-deposited film	30	33	1	20	16	-
BG3-4 as-deposited film	30	20	3	27	20	-

Table 4. Chemical compositions in at % for the BG target powders and for the BG films deposited onto titanium substrates. The values were determined by EDS for the films, and were calculated on the basis of the nominal oxides composition for the target.

The *in vitro* bioactivity of these BG samples, reflected in their capability of inducing HA-formation onto their surfaces, was investigated by immersion in SBF at 37°C for various periods of time up to 30 days. The SBF had the following ionic concentrations (in mM) of 142.0 Na⁺, 5.0 K⁺, 2.5 Ca²⁺, 1.5 Mg²⁺, 147.8 Cl⁻, 4.2 HCO³⁻, 1.0 HPO₄²⁻ and 0.5 SO₄²⁻, buffered at pH=7.4 with tris-hydroxymethyl-amminomethane (Tris, 50 mM) and hydrochloric acid solutions according to Kokubo (Kokubo & Takadama, 2006). A surface area to volume ratio of 0.1 cm⁻¹ was maintained for all immersions. The biomineralization processes at the BG-SBF interface were monitored, on the surface and in the volume, by FTIR, GIXRD and SEM. Hench's theory states that the first stage of a bioglass mineralization upon immersion in SBF involves the rapid exchange of Na⁺ and Ca²⁺ ions from the glass for H⁺ and H₃O⁺ ions from the solution, which will initialize the hydrolysis of the Si-O-Si bonds of the glass structure and the forming of silanol groups. The dissolution of the glass network, leading to the formation of silica-rich gel layer, the supersaturation of SBF solution with respect to hydroxyapatite and the subsequent deposition of an apatite-like layer on the glass surface, were found to be essential steps in the bioactivity evaluation both *in vivo* and *in vitro* studies (Hench, 1991). The formation of stable, mechanically strong interface with both bone and soft connective tissues is essential for the clinical success.

FTIR spectroscopy is a powerful method to obtain useful information concerning the short-range order for the as-deposited amorphous films as well as for SBF tested films, allowing the identification of specific features in the IR vibrational spectrum, such as those related to silicate or phosphate groups.

Figure 6 shows the FTIR spectra of the as-deposited and heat-treated BG films together with the spectra of the cathode target powder. Similar absorption envelopes for the target and as-deposited BG films have been recorded, exhibiting the same broad IR bands typical to an amorphous structure. However all the as-deposited BG films presents a shift to higher wave numbers of the maximum absorption peak with respect to the powder spectrum which indicate a certain degree of modification of the silicate tetrahedron network during sputtering, in good correlation with the compositional modification.

In case of BG1 structures (*Fig. 6-a*) we noted the presence of three intense vibration bands:

- 1001-1030 cm^{-1} assigned to asymmetric stretching vibrations of Si-O-Si in the Q² and Q³ units;
- 1102-1130 cm^{-1} , more intense for the as-deposited samples could be attributed to the anti-symmetric stretching mode of Si-O-Si groups;
- 794 cm^{-1} correspond to the bending motion of Si-O-Si links (Socrates, 2001; Agathopoulos et al., 2006).

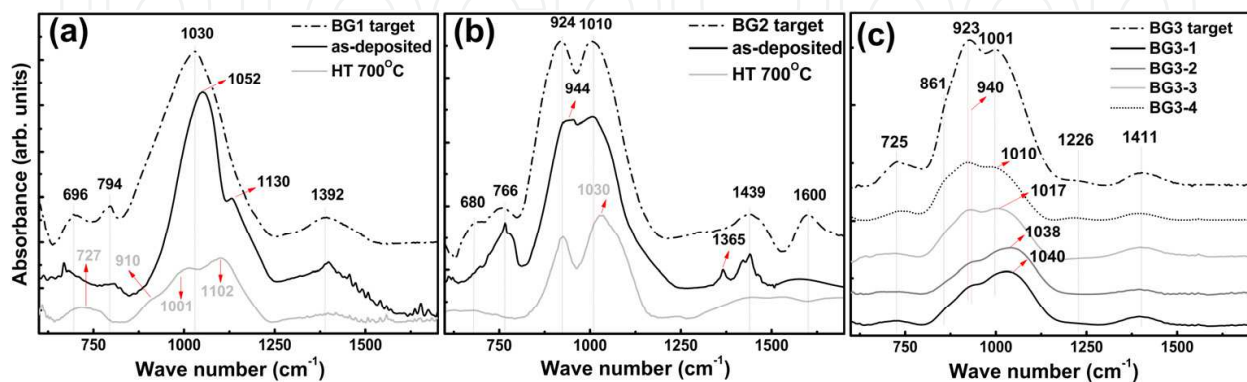


Fig. 6. Comparative FTIR spectra for the target powders and the studied films: a) BG1; b) BG2; c) BG3

The peak at 1383 cm^{-1} might be assigned to a shifted $(\text{CO}_3)^{2-}$ stretching band. The presence of the weaker band at 696 cm^{-1} corresponds to symmetric stretching bands of PØP Q³ in Q² and Q¹ units. After the heat-treatment at 700°C/2h one can observe the splitting of the envelope in two shoulders, indicating a crystallization of the BG structure, along with the appearance of new vibration band at 910 cm^{-1} (the stretching of the Si-O-3NBO and Si-O-2NBO) groups). A strong shift to lower wave numbers of the bands positioned at 1030 and 1120 cm^{-1} was also noticed.

The IR spectra of BG2 structures (*Fig. 6-b*) revealed three strong vibration bands:

- 924-944 cm^{-1} - attributed to the stretching vibration of the SiO₄ units with three and two non-bridging oxygen atoms, the Q¹ (Si-O-3NBO), and Q² (Si-O-2NBO) groups;
- 1010-1022 cm^{-1} assigned to the coexistence of various Q² and Q³ Si-O-Si asymmetric stretching vibration;
- 766 cm^{-1} correspond to the bending motion of Si-O-Si links (Socrates, 2001; Agathopoulos et al., 2006).

The weaker band at 680 cm^{-1} might correspond to symmetric stretching bands of PØP Q³ in Q² and Q¹ units. Other vibrations of phosphate groups present in the bioglass are difficult to emphasize because of the superimposition of the strong bands of SiO₄ units. Previous IR studies noticed also the presence of Q², Q¹, and Q⁰ phosphate units in the 1400–400 cm^{-1} IR spectra range (Socrates, 2001; Agathopoulos et al., 2006). The weak broad shoulder present at 1600 cm^{-1} can be assigned to water bending vibrations, indicating that BG1 material is highly hygroscopic, absorbing water vapour when in air. The presence of absorption band at 1439 cm^{-1} is attributed to the stretching vibrations of carbonate $(\text{CO}_3)^{2-}$ structures incorporated during the deposition process. After the post-deposition annealing a clear

splitting of the bands was noticed, pointing a strong crystallization of the BG coating, in agreement with the GIXRD measurements (Figs. 1 and 4).

All the BG3 films FTIR spectra displayed as weak broad absorption bands: two dominant peak maxima at $\sim 1030\text{ cm}^{-1}$ (Si-O stretching in Q^2 and Q^3 units) and at $\sim 940\text{ cm}^{-1}$ (Si-O stretching in Q^1 and Q^2 units). The weak shoulder at $\sim 725\text{ cm}^{-1}$ corresponds to Si-O-Si bending motion. Broad vibration bands centred at 1218 and 1411 cm^{-1} were evidenced, and are related to B-O stretching of BO_3 units in borates with bridging oxygen, vibrations of metaborate triangles and B-O stretching of $B\text{O}_4$ and $B\text{O}_2^-$ units (Agathopoulos et al., 2006).

In case of BG3 films the FTIR analysis revealed a dependence between argon deposition pressure and the short range order of the sputtered glass structure. The displacement of the asymmetric stretching vibration present at 1040 cm^{-1} (BG3-1) to lower wave numbers (Fig. 6-c) indicates the Si-O-Si linkages perturbation by a continuous formation of non-bridging oxygen type linkages with the increase of argon sputtering pressure, and the weakening of the structural bonds sustained by the bridging oxygen atoms (Fig. 6-c). The FTIR spectra displayed indeed an increase of the intensity ratio of the bands: $923\text{--}944\text{ cm}^{-1} / 1010\text{--}1040\text{ cm}^{-1}$, which denote the enrichment in Q^1 and Q^2 structural groups, with increasing the deposition pressure. This suggests that as the deposition pressure increases a higher concentration of alkali and alkali-earth oxides might be incorporated in the glass structure, the Q^3 groups being progressively converted to Q^2 groups (Socrates, 2001; Serra et al., 2002). A direct correlation between the glass thin films' composition and their structure that reflects directly in their biomineralization capability was reported in literature (Serra et al., 2002).

3.2 Bioactivity tests: Observations & considerations

Figure 7 displays a comparison of the BG films IR spectra before and after immersion in simulated body fluid up to 30 days.

For the as-deposited and annealed BG1 structures, the FTIR measurements (Fig. 7-a,b) showed no changes in intensity and position of the original vibration bands with immersion time, suggesting the inert character of this material.

In case of as-deposited BG2 samples (Fig. 7-c) after only 24 hours of immersion, dramatic changes were observed. The spectrum revealed the disappearance of the initial BG film vibration bands and the emergence of two new and strong bands positioned at 816 and 1107 cm^{-1} , which could be assigned to bending and stretching bands of the amorphous silica phase (Bal et al., 2001). Weaker bands at 736, 892 and 968 cm^{-1} , were noticed, belonging most probably to the original BG layer. The intensity of these bands decreased with the immersion time suggesting a continuously leaching of BG ions into the SBF solution. After 30 days of immersion the BG films is completely dissolved, no IR bands could be emphasized, indicating the resorbability of this material.

The FTIR results of the annealed BG2 samples after in-vitro testing in SBF are presented in Figure 3-d. After 24 hours soaking in SBF solution the amplitude of the peak at 924 cm^{-1} present increased values and displaced at $\sim 940\text{ cm}^{-1}$. This maximum peak at 940 cm^{-1} is

also present related to the Si-OH groups (Berbecaru et al., 2010). In comparison the peak positioned at 1030 cm^{-1} is decreased in amplitude. The process could be related to the continuous leaching of Na, Ca and Si ions in the SBF solution. The exchange of the ions between the surface layer and SBF solution lead to a rearranging of the bonds in the sample surfaces. At the same time the diffusion of the H^+ ions, because of the increase of the electronegativity of the surface toward the BG films will initiate the formation of the Si-OH bonds on their surface (L.L. Hench & J. Wilson, 2003; Berbecaru et al., 2010). The small shoulder at 895 cm^{-1} revealed the presence of the stretching vibrations of the Si-O bonds with two non-bridging oxygens (Q^1 and Q^0 units) from the original BG layer. After 72 hours of immersion in SBF solution the peaks at 776 and 1030 cm^{-1} increased in amplitude suggesting the enrichment of the Si-O-Si bonds in the SiO_4 tetrahedra (Q^4 units). This suggests that after a certain period of time the polymerization reaction begins at the film surface. Also, the peak at 940 cm^{-1} strongly decreases in amplitude, revealing three new weak bands at 960 cm^{-1} , 1021 and 1087 cm^{-1} respectively. These absorption bands are assigned to ν_1 symmetric stretching mode of $(\text{PO}_4)^{3-}$ (960 cm^{-1}) and to ν_3 asymmetric stretching of the phosphate groups, respectively (1021 and 1087 cm^{-1} bands) (Socrates, 2001).

This phenomena could be related to simultaneous phenomena such: formation of the silicic acid $\text{Si}(\text{OH})_4$ and subsequent polycondensation reaction, along with the beginning of the precipitation of calcium phosphate (Ca-P) phases on the surface from the SBF solution supersaturated in Ca-P ions (Berbecaru et al., 2010). The released water in the polycondensation reaction is known to remain physically bonded with the Si-O-Si surface forming the hydrated silica rich layer (Hench, 1991; L.L. Hench & J. Wilson, 2003). This is leading to an increase of the pH at the surface level which will be favourable to the absorption of the cations and anions on the surface, the precipitation processes of Ca-P rich phases being under these auspicious conditions.

The process of precipitation seems to continue up to 30 days, the relative integral area of the bands at 960 cm^{-1} , 1021 and 1087 cm^{-1} monotonously increasing with immersion time. Thus, it is suggested that on top of the annealed BG1 coatings chemically develops in vitro a Ca-P type layer. The broad aspect of the bands suggests the amorphous nature of this chemically grown layer. For comparison the spectrum of a crystalline synthetic hydroxyapatite powder is displayed. No crystallization processes were observed in XRD after 30 days of immersion.

Figure 7-e,f,g displays the evolution of the FTIR spectra for the BG3 structures after SBF immersions for 3, 15 and 30 days. Similar IR spectral evolutions were observed for all BG3 films. A change of the BG3 spectra envelope was noticed after 3 days of immersion in SBF (Fig. 7-e). There are some perceptible differences in shape and amplitude of the IR spectra between these three investigated glass films. The two dominant maxima (~ 1090 and $\sim 1120\text{ cm}^{-1}$, respectively) are assigned to the $(\text{PO}_4)^{3-}$ (ν_3) asymmetric stretching, hinting that after three days of immersion the precipitation of a Ca-P layer had started (G.E. Stan et al., 2011). A splitting of the phosphate stretching band, more clearly in case of BG3-4, could be observed, suggesting a more advanced stage of amorphous calcium phosphates phases' precipitation. Thus, at this point, one can deduce that partial dissolution of BG3 structures occurred up to 3 days, as demonstrated by the diminishing overall intensity of

the spectrum and the lower contribution of silicates bands overlapped by the emergence of dominant phosphate bands due to Ca-P precipitation. The leaching of BG ions along with the dissolution-diffusion of silicon atoms from the glass structure resulting in a supersaturation at the film-SBF interface is a prerequisite condition for the starting of precipitation process (Hench, 1991). One can hypothesize that the peak positioned at $\sim 1125\text{ cm}^{-1}$ could obscure also the presence of Si-O-Si asymmetric stretching vibrations (Hench, 1991; Socrates, 2001), owned to the silica-rich layer formed at the film-solution interface at an early stage (Hench, 1991). After 15 days (Fig. 7-f), all the BG3 samples displayed similar IR spectra, defined by the phosphate's two intense shoulders positioned around 1028 and 1121 cm^{-1} , respectively. Increases in intensity of water and O-H bands along with the appearance of $(\text{CO}_3)^{2-}$ stretching vibration bands suggest a continuous incorporation of various molecular structures at the liquid-solid interface. After 30 days of immersion the FTIR absorbance spectra (Fig. 7-g) revealed strong vibrations at the following wave numbers: 876 , 960 , 1019 , 1107 , 1413 , 1465 , and 1635 cm^{-1} , corresponding to crystalline carbonated apatite (CHA). The sharp bands at 1019 cm^{-1} and 1107 cm^{-1} correspond to (ν_3) asymmetric stretching of phosphate groups. The splitting of the stretching and bending IR absorption bands in two narrow components suggests a crystalline apatitic growth. The weak band centred at 960 cm^{-1} is assigned to $(\text{PO}_4)^{3-}$ (ν_1) symmetric stretching mode. All apatitic layers obtained were hydroxylated and carbonated as demonstrated by the presence of strong O-H bands (the bending mode centred at $\sim 1635\text{ cm}^{-1}$) and the sharp C-O bending (ν_2) and stretching (ν_3) lines at (876 , 1413 and 1465 cm^{-1}). Considering the hydroxyapatite structure, the carbonate group can substitute both the hydroxyl and the phosphate ions, giving rise to the A-type and B-type carbonation, respectively. The positions of the carbonate bands indicate that $(\text{CO}_3)^{2-}$ groups are substituting $(\text{PO}_4)^{3-}$ ions, suggesting the predominance of B-type CHA (Markovic et al, 2004). The B-type is the preferential substitution in the human bone and is known to have better bioactivity and osteoinductivity (Spence et al., 2008).

The GIXRD patterns are presented in Fig. 8 revealed after 30 days immersion in SBF the characteristic lines of hydroxyapatite (HA) as large, overlapping peaks (ICDD: 9-432, for instance) for all the samples. There are deviations of relative intensities with respect to the reference ICDD card, due probably to imperfect stoichiometry. The increased relative intensity of the (002) line is often reported for chemically grown HA layers and it is assigned to the preferred orientation of crystallites and is typical for the biological apatite. The HA peaks are broad due either to the small crystallite size or to lattice disorder or to both (G.E. Stan et al., 2011). The mean crystallite size along the c axis of the hexagonal HA structure, estimated from the (002) line broadening by using the Scherrer formula, is about 25-30 nm (strain-broadening neglected). Because of the large line broadening one can not distinguish between different HA types, for instance between HA and carbonated HA.

After three days of immersion in SBF a strong and narrow diffraction peak appeared in the GIXRD patterns of BG3-1, BG3-2 and BG3-3 at $2\theta = 26.5^\circ$, whose intensity is correlated with that of a weak line at $2\theta = 54.6^\circ$. The most plausible phase is calcium phosphate hydrate type (i.e. $\text{Ca}(\text{H}_2\text{P}_2\text{O}_7)$ ICDD: 70-6384), whose role in the subsequent HA formation has been the subject of several detailed studies (Liu et al., 2008).

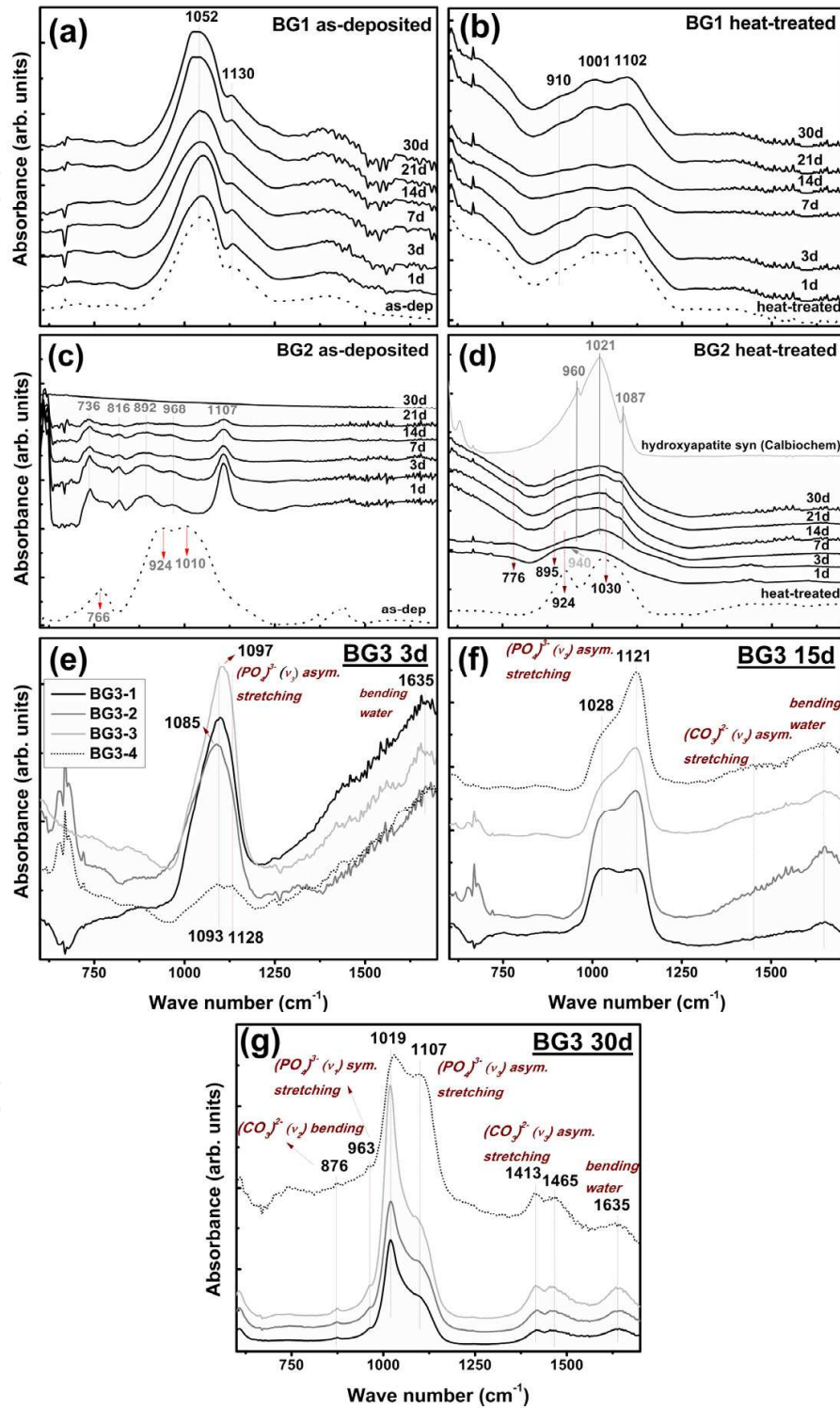


Fig. 7. Evolution of FTIR spectra of the BG films with increasing immersion time in SBF (1 - 30 days)

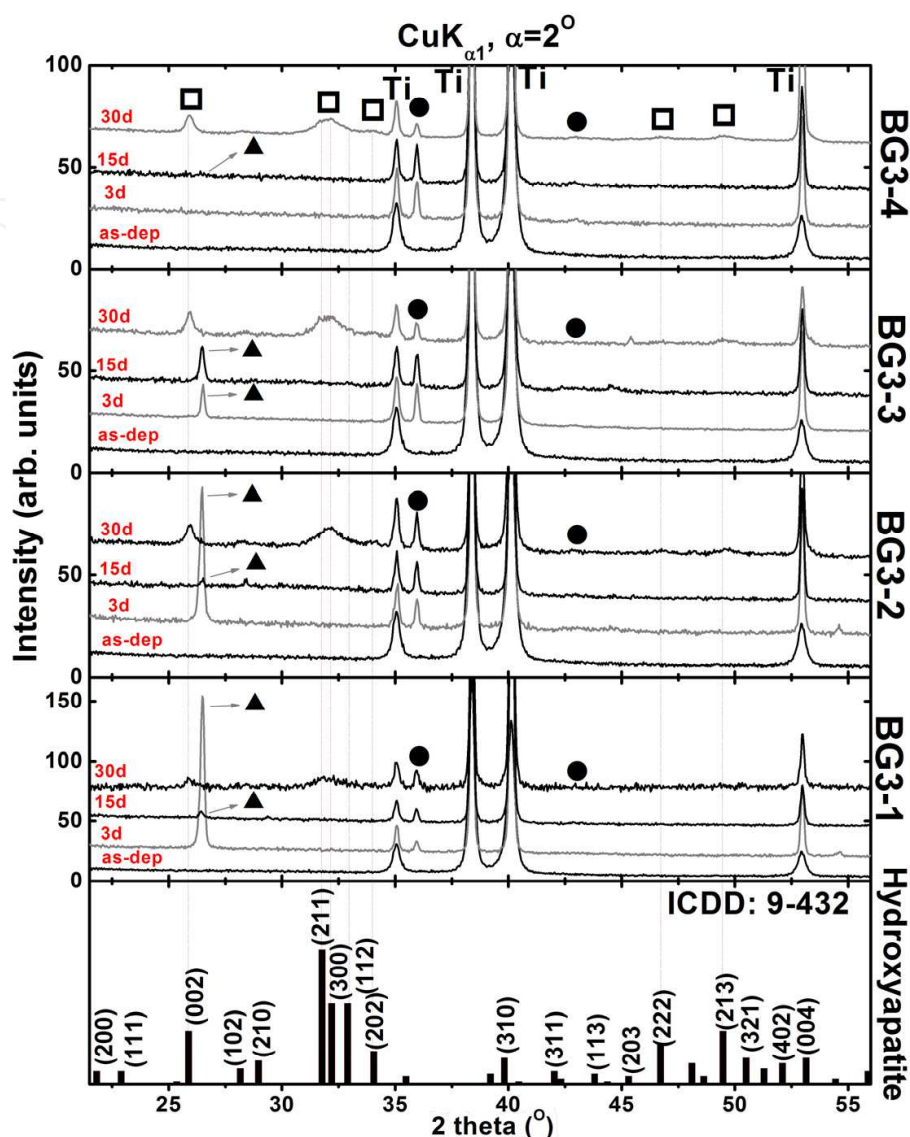


Fig. 8. Comparative representation of the GIXRD patterns of the as-deposited BG films before and after 3, 15 and 30 days immersion in SBF. □= Hydroxylapatite (ICDD:9-432); ●= $TiH_{1.7}$ (ICDD:40-1244); ▲ = calcium phosphate hydrate (ICDD: 70-6384)

The intensity of the line at $2\theta = 26.5^\circ$ start to diminish until the 15th day of immersion in SBF, and almost disappears after 30 days for all the samples. It is interesting to note that this phase has a strong intensity only in the structures deposited in pure Ar (BG3-1, BG3-2 and BG3-3) and it is very weak for the BG3-4 samples deposited in reactive atmosphere (7% oxygen). Another quite intensive line in the GIXRD patterns of the samples after SBF immersion appears at $2\theta = 36.0^\circ$. The best assignment for this line is TiH (ICDD: 40-1244). This peak is present in all the structures that were immersed in SBF and it is expected that its presence is related to the uncovered regions of the titanium substrate.

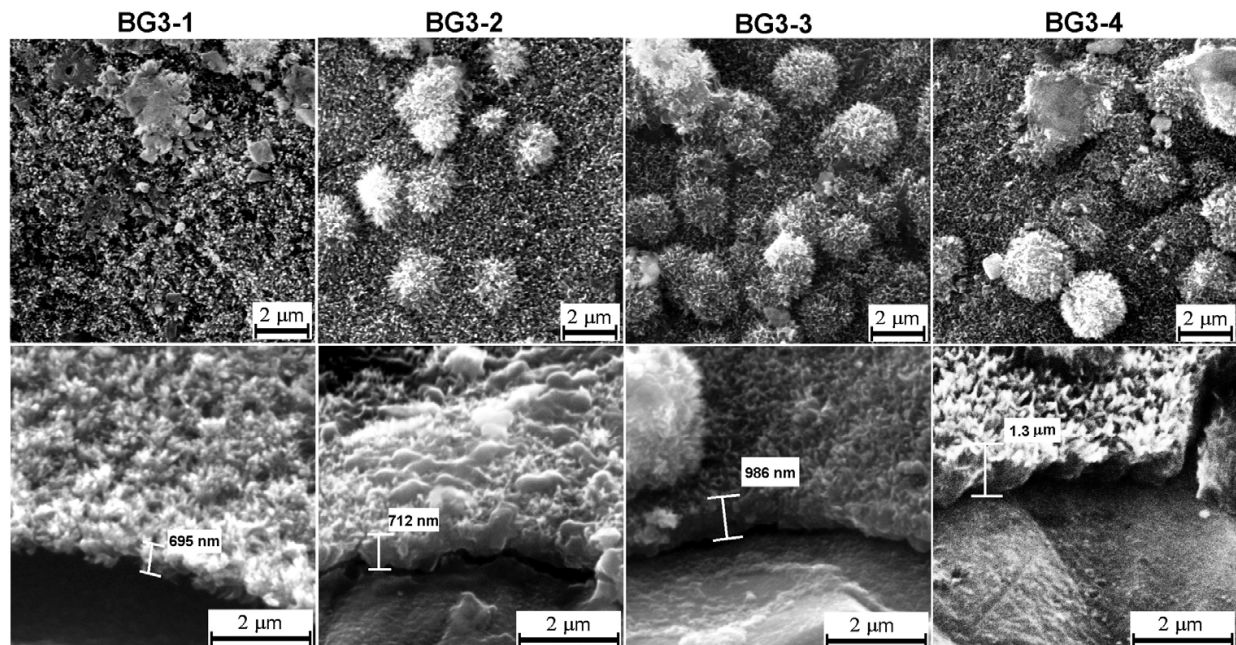


Fig. 9. SEM micrographs of BG3 films after immersion in SBF for 30 days. Left side, SEM-top view; Right side, ESEM-cross view

The SEM microstructures of BG3 films immersed for 30 days clearly asserted the growth of thick and rough coatings with randomly distributed irregular spherulitic shaped micro-sized agglomerates on top of all three types of samples, evidencing the good biomineralization capability of all coatings (Fig. 9-top row). The thicknesses of the chemical grown HA layers were determined by tilt-SEM (Fig. 9-bottom row). One can observe that the BG3-3 and BG3-4 coatings led to the thickest chemical growths: total film thickness $\sim 1 \mu\text{m}$, and $\sim 1.3 \mu\text{m}$, respectively, compared to the as-deposited film thickness of $\sim 0.4 \mu\text{m}$. The HA chemically grown layers had in case of BG3-1 and BG3-2 structures a lower average thickness of $\sim 0.7 \mu\text{m}$. Thus, the best biomineralization, correlated with the thickest HA layer growth, was obtained for the BG3-4 coating (G.E. Stan et al., 2011).

3.3 Discussion

Thus, the IR spectra of the samples immersed in SBF for 1 month showed different behaviour *in vitro* as a function of composition and crystallization state.

The inertness of BG1 structures might be determined by their chemical composition. High contents of SiO_2 have influences both in bioactivity and the thermal expansion coefficient of the glass. In general, SiO_2 -rich glasses with silica contents higher than 60 wt.% have a better mechanical stability and adhesion to the metallic substrate, but are not soluble in body fluids (Lopez-Esteban et al., 2003). Decreasing the silica content is therefore mandatory for improving the bioactivity and partial dissolution of the glass surface. For the BG1 structures one can notice an important silicon ($\sim 50 \text{ at.}\%$) and phosphorous content ($\sim 10 \text{ at.}\%$). In silica-based glasses phosphorous acts as a network former producing structural rearrangement where the silicate network is more interconnected by creating P-O-Si cross-links. At higher content of phosphorus, the glass is increasing in connectivity. The glass compositions with higher content of network formers, do not bond either to bone or to soft tissues and elicit

formation of a non-adherent fibrous interfacial capsule. No surface changes during SBF tests were evidenced for the annealed BG1 structure. Unlike in case of BG2, the crystallization had no effect on BG1's surface reactivity. The nucleated $\text{Na}_2\text{Mg}(\text{PO}_3)_4$ phase proved to be inert in SBF. It can be concluded that the chemical composition, bonding configuration and crystallinity could play important roles in BG films' reactivity in SBF.

In case of as-deposited BG2 samples a continuous dissolution process occurs, after 30 days the entire film is dissolved into the surrounding fluid. One can notice the high content of Ca (~20 at.%) and Na atoms (~43 at.%) in the BG2 film (Table 3). It can be speculated that when very high numbers of alkali and alkali-earth ions are released in SBF, the pH will rapidly and drastically change at the film-fluid interface, producing a chemical unbalance which will suppress the polymerization of silanols and the further formation of the SiO_2 -rich surface layer. The bioactive process is thus disrupted, leading to continuous dissolution of the BG amorphous film. On the other hand the annealing of BG1 films followed by slow cooling promotes formation of combeite, wollastonite and Na_3PO_4 , which have smaller solubility, and consequently a decreased leaching rate of Na^+ and Ca^{2+} into the SBF solution. This will determine the conditions at the surface of the film to be more stable, therefore allowing polymerisation of soluble $\text{Si}(\text{OH})_4$ in a SiO_2 -rich layer which will act as a nucleation site for apatite (L.L. Hench & J. Wilson, 2003). During 30 days of SBF soaking, dissolution-reprecipitation processes took place, the annealed BG2 layer is partially dissolved and finally we obtain a multilayer structure containing a bottom BG layer coated by an amorphous SiO_2 -rich thin film and at the top a Ca-P type layer. Thus in case of BG2 annealed samples our FTIR results are consistent with Hench's theory. Previous studies have also reported that both the combeite (Chen et al., 2006) and wollastonite (Xue et al., 2005) can generate on their surface Ca/P rich layers when in contact with SBF. The growth of the bioapatite layer is essential for bone generation and bonding ability. However, the combeite was proved to rapidly transform into amorphous calcium phosphate phase in contact with SBF, but it delays the process of crystallization into a hydroxyapatite phase (L.L. Hench & J. Wilson, 2003). Besides biocompatibility, these structures could actively improve proteins and osteocytes adhesion, significantly shortening the osteointegration time.

Regarding the higher biomineralization rates of BG3-3 and BG3-4 films one can hypothesize that the chemical processes involved in the bioactivity mechanism are accelerated, because of the increased sodium content of these films and a propitious bridging oxygen/non-bridging oxygen ratio (Table 4), speeding up the ionic exchange and the chemical growth of HA. Hench's theory states that the first stage of SBF immersion of a bioglass involves the rapid exchange of Na^+ ions from the glass for H^+ and H_3O^+ ions from the solution, which shall initialize the formation of silica-rich layer known to favour the nucleation of Ca-P type layers. Therefore, we can suppose that a higher number of sodium ions released into SBF solution will change the chemical equilibrium of the precipitation reaction, thereby catalyzing the CHA chemical growth mechanism.

Therefore, for achieving bioactive properties, an optimal ratio of network formers/network modifiers is required, but not sufficient. The disruption of the Si-O-Si bonds and creation of Si-O-NBO bonds, determined by increased network modifiers content, is mandatory in the first steps of Ca-P chemical growth mechanism. The disruption of the Si-O-Si bonds evidenced by the increasing content of Si-O-NBO groups plays an important role in the

dissolution rate of silica in the first steps of Hench's chemical growth mechanism, favouring the bioactivity processes of the films by a higher rate of biomineralization (Serra et al., 2002; Liste et al., 2004). This hypothesis is in agreement with our results, the stronger biomineralization, expressed by the thickest CHA film grown, was obtained for the BG3 sample. Although BG compositions with very high network modifier content have a native poor stability, we can tailor their in-vitro behaviour by thermal treatments of crystallization to obtain the best bioactive outcome (G.E. Stan et al., 2010b).

The mechanism of calcium phosphates formation onto the surface of bioactive glasses is widely accepted, and involves the dissolution of cations from the surface of bioactive glasses and the consequent increase of the supersaturation degree in the surrounding fluid, with respect to HA components. Hench's theory states that the first stage of a bioglass mineralization upon immersion in SBF involves the rapid exchange of Na^+ ions from the glass for H^+ and H_3O^+ ions from the solution, which shall initialize the breaking of the Si-O-Si bonds of the glass structure and the subsequent formation of silanol groups. In a next step the silanol groups polycondensate forming a silica-rich layer at the bioglass surface, which favours the growth of Ca-P type layers. Homogenous nucleation (precipitation) of biomimetic apatite occurs spontaneously in a solution supersaturated with respect to hydroxyapatite. Heterogeneous precipitation, on the other hand, takes place on the sample's surface. Both, homogenous and heterogeneous nucleation, could be considered in competition during the SBF immersion.

Due to their designed low thickness (lower than 700 nm), even in case of total dissolution, the amount of BG film that could be released in the SBF solution is around few micrograms. Thus, intuitively the bioactivity processes will not be governed in case of thin BG films preponderantly by the supersaturation of SBF solution in Na, Ca and P and further precipitation of Ca-P phases, but by the pH evolution at the sample-solution interface, surface energy and electrostatic interactions between electrically negative charged sample surface and the cations and anions from stagnant solution in the proximity of the BG surface.

A reinterpretation of the classical biomineralization process based on the electrical double layer effect will be presented. The electrical double layer refers to two parallel layers differing in charge surrounding an object (BG sample). The increased number of surface hydroxyl groups could act as nucleation sites for HA. Thus the first layer, with negative surface charge, comprises Si-OH⁻ groups primarily formed during chemical interactions with the fluid. Ca^{2+} ions and with them also anions, such as $(\text{HPO}_4)^{2-}$, are present in the electrolyte space charge facing the sample surface enriched in polymerising silanol groups. Thus, the second layer is composed of calcium ions attracted to the surface charge via the Coulomb force, electrically screening the first layer. This second layer could be seen in the first stages as a diffuse layer being loosely connected with the silica-rich one, as it consists of free calcium ions which move in the fluid under the influence of electric attraction and thermal motion. As the $(\text{HPO}_4)^{2-}$ anions interact and react with this second layer, the heterogeneous nucleation of CaO-P₂O₅ layer starts, which is anchoring progressively into the sample's surface, resulting in a hydrated precursor cluster consisting of calcium hydrogen phosphate, and in time by consuming and incorporating various ions [(OH)⁻, F⁻ or (CO₃)²⁻] from the surrounding media crystallize into a carbonated-flour-hydroxyapatite mixed layer. Consequently in case of BG thin films one should consider the heterogeneous nucleation as the dominant mechanism of HA growth.

4. Conclusions

The effects of sputtering pressure, composition of working atmosphere and deposition parameters on the compositional, morpho-structural and mechanical properties of the coated implants were emphasized, and their influence on the *in vitro* behaviour of the coatings in simulated body fluid (SBF) was studied.

The adhesion strength at the coating – substrate interface is a critical factor in successful implantation and long-term stability of such implant-type structures. The chapter presented few technological RF-MS derived approaches to surpass the low adherence drawback when dealing with BG having high CTE: by introducing intermediate buffer layers [BG_{1-x}Ti_x (x=0-1)] with compositional gradient, or by strong inter-diffusion phenomena induced via heat-treatments, with the aim in the nucleation of BG-Ti mix phases at the substrate-coating interface. The importance of a proper *in situ* substrate cleaning, performed by argon ion sputtering processes which will enhance the ad-atoms diffusion, should be also emphasized. Also when using BG cathode target with CTE closely matching the Ti substrates, the RF-MS deposition conditions exert great influence on the adherence of films as well as on their composition. The application of the above mentioned technological algorithms conducted to pull-out adhesion values higher than the usual ones reported in literature, opening new perspectives in oral and orthopaedic implantology.

Peculiarities of the *in vitro* behaviour of the BG thin films were discussed in correlation with the widely accepted Hench bioactivity mechanism. Based on our *in vitro* studies it was concluded that the chemical composition, bonding configuration and crystallinity could play important roles in BG films' reactivity in SBF. For achieving bioactive properties an optimal ratio of network formers/network modifiers is a necessary, but not sufficient, condition. BG compositions with very high network modifier content have a poor native stability, and their *in vitro* behaviour can be tailored by thermal treatments of crystallization to obtain the best biological outcome.

By varying the sputtering pressure and working atmosphere we attempted to tailor the films' composition and structure, hinting optimal mechanical performance and bioactive behaviour. Understanding these correlations is important for biomaterials science, implantology, as well as from an applied physics and technological point of view, opening new perspectives in regenerative medicine.

5. Acknowledgments

The financial support of Centre for Research in Ceramics and Composites (CICECO) – University of Aveiro and of the Romanian Ministry of Education, Research, Youth and Sport (Core Program – Contract PN09-45) is gratefully acknowledged. Authors thank Dr. Iuliana Pasuk for the professional assistance with GIXRD measurements.

6. References

Agathopoulos, S.; Tulyaganov, D.U.; Ventura, J.M.G.; Kannan, S.; Karakassides, M.A. & Ferreira J.M.F. (2006). Formation of hydroxyapatite onto glasses of the CaO–MgO–

- SiO₂ system with B₂O₃, Na₂O, CaF₂ and P₂O₅ additives. *Biomaterials*, Vol.27, No.9, (March 2006), pp. 1832–1840, ISSN 0142-9612
- Alcock, C.B. (2001). *Thermochemical Processes – Principles and Models*, Butterworth-Heinemann, ISBN 0-7506-5155-5, Oxford, UK
- American Society for Testing and Materials [ASTM]. (2009). *Standard specification for composition of ceramic hydroxylapatite for surgical implants F 1185-03*, pp. 514-515
- Bal, R.; Tope, B.B.; Das, T.K.; Hegde, S.G. & Sivasanker, S. (2001). Alkali-loaded silica, a solid base: Investigation by FTIR Spectroscopy of adsorbed CO₂ and its catalytic activity. *Journal of Catalysis*, Vol.204, No.2, (December 2001), pp. 358–363, ISSN 0021-9517
- Balamurugan, A.; Balossier, G.; Kannan, S.; Michel, J.; Rebelo, A.H.S. & Ferreira J.M.F. (2007). Development and in vitro characterization of sol-gel derived CaO-P₂O₅-SiO₂-ZnO bioglass. *Acta Biomaterialia*, Vol.3, No.2, (March 2007), pp. 255–262, ISSN 1742-7061
- Batchelor, A.W. & Chandrasekaran, M. (2004). *Service characteristics of biomedical materials and implants*, Imperial College Press, ISBN 1-86094-475-2, London, UK
- Berbecaru, C.; Alexandru, H.V.; Stan, G.E.; Marcov, D.A, Pasuk, I. & Ianculescu, A. (2010). First stages of bioactivity of glass-ceramics thin films prepared by magnetron sputtering technique. *Materials Science and Engineering B: Solid-State Materials for Advanced Technology*, Vol.168, No.1-3, (May 2010), pp. 101-105, ISSN 0921-5107
- Berezhnaya, A. Yu.; Mittova, V.O.; Kostyuchenko, A.V. & Mittova, I. Ya. (2008). Solid-phase interaction in the hydroxyapatite/titanium heterostructures upon high-temperature annealing in air and argon. *Inorganic Materials*, Vol.44, No.11, (November 2008), pp. 1214–1217, ISSN 0020-1685
- Berg, S. & Nyberg, T. (2005). Fundamental understanding and modeling of reactive sputtering processes. *Thin Solid Films*. Vol. 476, No.2, (April 2005), pp. 215-230, ISSN 0040-6090
- Brown, C.; Papageorgiou, I.; Fisher, J.; Ingham, E. & Case, C.P. (2006). Investigation of the potential for wear particles generated by metal-on-metal and ceramic-on-metal implants to cause neoplastic changes in primary human fibroblasts. *Journal of Bone & Joint Surgery (British Volume)*, Vol. 88-B, SUPP III, pp. 393, ISSN 0301-620X
- Brown, C.; Williams, S.; Tipper, J.L.; Fisher, J. & Ingham E. (2007). Characterisation of wear particles produced by metal on metal and ceramic on metal hip prostheses under standard and microseparation simulation. *Journal of Materials Science: Materials in Medicine*, Vol.18, No.5, (May 2007), pp. 819–827, ISSN 0957-4530
- Chen, Q.Z.; Thompson, I.D. & Boccaccini, A.R. (2006). 45S5 Bioglass®-derived glass-ceramic scaffolds for bone tissue engineering. *Biomaterials*, Vol.27, No.11, (April 2006), pp.2414-2425, ISSN 0142-9612
- Draft International Standards [ISO/DIS]. (1999). *Implants for surgery – Hydroxyapatite ceramic*. Part 1 and 2, pp. 13779
- El Batal, H.A.; Azooz, M.A.; Khalil, E.M.A.; Soltan Monem, A. & Hamdy, Y.M. (2003). Characterization of some bioglass-ceramics. *Materials Chemistry and Physics*, Vol.80, No.3, (June 2003), pp. 599-609, ISSN 0254-0584

- Elgayar, I.; Aliev, A.E.; Boccaccini, A.R. & Hill, R.G. (2005). Structural analysis of bioactive glasses. *Journal of Non-Crystalline Solids*, Vol.351, No.2 (January 2005), pp. 173–183, ISSN 0022-3093
- Epinette, J.A.; Manley, M.T.; Geesink, R.G.T. (2003). *Fifteen years of clinical experience with hydroxyapatite coatings in joint arthroplasty*, Springer-Verlag, ISBN 2-287-00508-0, Paris, France
- Food and Drug Administration [FDA]. (1997). *Calcium phosphate (Ca-P) coating draft guidance for preparation of FDA submissions for orthopedic and dental endosseous implants*, pp. 1-14
- Goller, G. (2004). The effect of bond coat on mechanical properties of plasma sprayed bioglass-titanium coatings. *Ceramic International*, Vol.30, No.3, pp. 351–355, ISSN 0272-8842
- Hench, L.L. (1991). Bioceramics: From concept to clinic. *Journal of American Ceramic Society*, Vol.74, No.7, (July 1991), pp. 1487–1510, ISSN 0002-7820
- Hench, L.L. & Wilson, J. (1993). *Introduction to Bioceramics*, World Scientific, ISBN 981-02-1400-6, Singapore, Singapore
- Kokubo, T. & Takadama, H. (2006). How useful is SBF in predicting in vivo bone bioactivity?. *Biomaterials*, Vol.27, No.15, (May 2006), pp. 2907-2915, ISSN 0142-9612
- Lacefield, W.R. (1988). Hydroxyapatite coatings. In: *Bioceramics: material characteristics versus in vivo behavior*, Ducheyne, P. & Lemons, J.E., Vol. 523, pp. 72–80, Annals of the New York Academy of Science, ISBN 978-0-89766-437-0, New York, USA
- Lefebvre, L.; Chevalier, J.; Gremillard, L.; Zenati, R.; Pollet, G.; Bernache-Assolant, D. & Govin, A. (2007). Structural transformations of bioactive glass 45S5 with thermal treatments. *Acta Materialia*, Vol.55, No.10, (June 2007), pp. 3305-3313, ISSN 1359-6454
- Liste, S.; Serra, J.; González, P.; Borrajo, J.P.; Chiussi, S.; León, B. & Pérez-Amor, M. (2004). The role of the reactive atmosphere in pulsed laser deposition of bioactive glass films. *Thin Solid Films*, Vol.453 -454, (April 2004), pp. 224–228, ISSN 0040-6090
- Liu, X.; Zhao, X.; Li, B.; Cao, C.; Dong, Y.; Ding, C.; Chu, P.K. (2008). UV-irradiation-induced bioactivity on TiO₂ coatings with nanostructural surface. *Acta Biomaterialia*. Vol. 4, No.3, (May 2008), pp. 544 - 552, ISSN 1742-7061
- Lopez-Esteban, S.; Saiz, E.; Fujino, S.; Oku, T.; Suganuma, K. & Tomsia, A.P. (2003). Bioactive glass coatings for orthopedic metallic implants. *Journal of European Ceramic Society*, Vol.23, No.15, pp. 2921-2930, ISSN 0955-2219
- Mardare, C.C.; Mardare, A.I.; Fernandes, J.R.F.; Joannia, E.; Pina, S.C.A.; Fernandes, M.H.V.; & Correia R.B. (2003). Deposition of bioactive glass-ceramic thin-films by RF magnetron sputtering. *Journal of European Ceramic Society*, Vol.23, No.7 (June 2003), pp. 1027–1030, ISSN 0955-2219
- Markovic, M.; Fowler, B.O. & Tung, M.S. (2004). Preparation and comprehensive characterization of a calcium hydroxyapatite reference material. *Journal of Research of the National Institute of Standards and Technology*, Vol. 109, No.6, (November 2004), pp. 553-568, ISSN 1044-677X

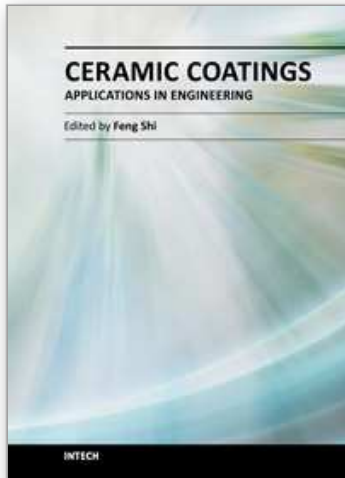
- Mattox, D.M. (1994). Surface Engineering. In: *ASM Handbook*, Reidenbach, F., Vol. 5, pp. 538, ASM International, ISBN 978-0-87170-384-2
- Palmero, A.; Rudolph, H. & Habraken, F.H.P.M. (2007). One-dimensional analysis of the rate of plasma-assisted sputter deposition. *Journal of Applied Physics*, Vol.101, No.8, art.no. 083307 (6 pages), ISSN 0021-8979
- Peitl Filho, O.; LaTorre, G.P. & Hench, L.L. (1996). Effect of crystallization on apatite-layer formation of bioactive glass 45S5. *Journal of Biomedical Materials Research*, Vol.30, No.4 (April 1996), pp. 509-514, ISSN 1549-3296
- Peddi, L.; Brow, R.K. & Brown, R.F. (2008). Bioactive borate glass coatings for titanium alloys. *Journal of Materials Science: Materials in Medicine*, Vol.19, No.9, (September 2008), pp. 3145-3152, ISSN 0957-4530
- Rámila, A. & Vallet-Regí, R.M. (2001). Static and dynamic in vitro study of a sol-gel glass bioactivity. *Biomaterials*, Vol.22, No.16, (August 2001), pp. 2301-2306, ISSN 0142-9612
- Ratner, B.D.; Hoffman, A.S.; Schoen, F.J. & Lemons, J.E. (2004). *Biomaterials Science: An Introduction to Materials in Medicine*. Elsevier Academic Press, ISBN 0-12-582463-7, San Diego, USA
- Saino, E.; Maliardi, V.; Quartarone, E.; Fassina, L.; Benedetti, L.; De Angelis, M.G.; Mustarelli, P.; Facchini, A. & Visai, L. (2010). In vitro enhancement of SAOS-2 cell calcified matrix deposition onto radio frequency magnetron sputtered bioglass-coated titanium scaffolds. *Tissue Engineering Part A*, Vol.16, No.3, (March 2010), pp. 995-1008, ISSN 1937-3341
- Saravanapavan, P. & Hench, L.L. (2001). Low-temperature synthesis, structure, and bioactivity of gel-derived glasses in the binary CaO-SiO₂ system. *Journal of Biomedical Materials Research*, Vol.54, No.4, (March 2001), pp. 608-618, ISSN 1549-3296
- Sepulveda, P.; Jones, J.R. & Hench L.L. (2002). Bioactive sol-gel foams for tissue repair. *Journal of Biomedical Materials Research*, Vol.59, No.2, (February 2002), pp. 340-348, ISSN 1549-3296
- Serra, J.; González, P.; Liste, S.; Chiussi, S.; León, B.; Pérez-Amor, M.; Ylänen, H.O.; Hupa, M. (2002). Influence of the non-bridging oxygen groups on the bioactivity of silicate glasses. *Journal of Materials Science: Materials in Medicine*, Vol.13, No.12, (December 2002), pp. 1221-1225, ISSN 0957-4530
- Socrates, G. (2001). *Infrared and Raman Characteristic Group Frequencies – Tables and Charts*, John Wiley & Sons Inc., ISBN 978-0-470-09307-8, Hoboken, USA
- Spence, G.; Phillips S.; Campion, C.; Brooks, R. & Rushton, N. (2008). Bone formation in a carbonate-substituted hydroxyapatite implant is inhibited by zoledronate. The importance of bioresorption to osteoconduction. *Journal of Bone & Joint Surgery (British Volume)*, vol. 90B, No.12, pp. 1635-1640, ISSN 0301-620X
- Stan, G.E.; Morosanu, C.O.; Marcov, D.A.; Pasuk, I.; Miculescu, F. & Reumont, G. (2009). Effect of annealing upon the structure and adhesion properties of sputtered bio-glass/titanium coatings. *Applied Surface Science*, Vol.255, No.22, (August 2009), pp. 9132-9138, ISSN 0169-4332

- Stan, G.E.; Pina, S.; Tulyaganov, D.U.; Ferreira, J.M.F.; Pasuk, I. & Morosanu, C.O. (2010). Biomineralization capability of adherent bio-glass films prepared by magnetron sputtering. *Journal of Materials Science: Materials in Medicine*, Vol.21, No.4, (April 2011), pp. 1047-1055, ISSN 0957-4530
- Stan, G.E.; Popa, A.C. & Bojin, D. (2010). Bioreactivity evaluation in simulated body fluid of magnetron sputtered glass and glass-ceramic coatings: A FTIR spectroscopy study. *Digest Journal of Nanomaterials and Biostructures*, Vol.5, No.2, (April-June 2010), pp. 557-566, ISSN 1842-3582
- Stan, G.E.; Popescu, A.C.; Mihailescu, I.N.; Marcov, D.A.; Mustata, R.C.; Sima, L.E.; Petrescu, S.M.; Ianculescu, A.; Trusca, R. & Morosanu, C.O. (2010). On the bioactivity of adherent bioglass thin films synthesized by magnetron sputtering techniques. *Thin Solid Films*, Vol.518, No.21, (August 2010), pp. 5955-5964, ISSN 0040-6090
- Stan, G.E.; Marcov, D.A.; Pasuk, I; Miculescu, F; Pina, S.; Tulyaganov, D.U. & Ferreira, J.M.F. (2010). Bioactive glass thin films deposited by magnetron sputtering technique: The role of working pressure. *Applied Surface Science*, Vol.256, No.23, (September 2010), pp. 7102-7110, ISSN 0169-4332
- Stan, G.E.; Pasuk, I.; Husanu, M.A.; Enculescu, I.; Pina, S.; Lemos, A.F.; Tulyaganov, D.U.; El Mabrouk, K. & Ferreira, J.M.F. (2011). Highly adherent bioactive glass thin films synthesized by magnetron sputtering at low temperature. *Journal of Materials Science: Materials in Medicine*, Vol.22, No.12, (December 2011), pp. 2693-2710, ISSN 0957-4530
- Tulyaganov, D.U.; Agathopoulos, S.; Valerio, P.; Balamurugan, A.; Saranti, A.; Karakassides, M.A. & Ferreira, J.M.F. (2011). Synthesis, bioactivity and preliminary biocompatibility studies of glasses in the system CaO-MgO-SiO₂-Na₂O-P₂O₅-CaF₂. *Journal of Materials Science: Materials in Medicine*, Vol.22, No.2 (February 2011), pp. 217-227, ISSN 0957-4530
- Vallet-Regí, R.M.; Ragel, C.V. & Salinas, A.J. (2003). Glasses with medical applications. *European Journal of Inorganic Chemistry*, Vol.2003, No.6, (March 2003), pp. 1029-1042, ISSN 1434-1948
- van Hattum, E.D.;Palmero, A.; Arnoldbik, W.M.;Rudolph, H & Habraken, F.H.P.M. (2007). On the ion and neutral atom bombardment of the growth surface in magnetron plasma sputter deposition. *Applied Physics Letters*, Vol. 91, Art.no. 171501 (3 pages), ISSN 0003-6951
- Wasa, K.; Kitabatake, M. & Adachi, H. (2004). *Thin Film Materials Technology: Sputtering of Compound Materials*, Springer-Verlag, ISBN 3-540-21118-7, Heidelberg, Germany
- Wei, M.; Ruys, A.J.; Swain, M.V.; Milthorpe, B.K. & Sorrell, C.C. (2005). Hydroxyapatite-coated metals: Interfacial reactions during sintering. *Journal of Materials Science: Materials in Medicine*, Vol.16, No.2, (February 2005), pp. 101-106, ISSN 0957-4530
- Wolke, J.G.C.; van den Beucken, J.J.J.P. & Jansen, J.A. (2008). Growth behavior of rat bone marrow cells on RF magnetron sputtered bioglass- and calcium phosphate coatings. *Key Engineering Materials*, Vol.361-363, pp. 253-256, ISSN 1662-9795

- Wu, Z.Y.; Hill, R.G.; Yue, S.; Nightingale, D.; Lee, P.D. & Jones, J.R. (2011). Melt-derived bioactive glass scaffolds produced by a gel-cast foaming technique. *Acta Biomaterialia*, Vol.7, No.4, (April 2011), pp. 1807-1816, ISSN 1742-7061
- Xue, W.; Liu, X.; Zheng, X. & Ding, C. (2005). In vivo evaluation of plasma-sprayed wollastonite coating. *Biomaterials*, Vol.26, No.17, (June 2005), pp. 3455-3460, ISSN 0142-9612

IntechOpen

IntechOpen



Ceramic Coatings - Applications in Engineering

Edited by Prof. Feng Shi

ISBN 978-953-51-0083-6

Hard cover, 286 pages

Publisher InTech

Published online 24, February, 2012

Published in print edition February, 2012

The main target of this book is to state the latest advancement in ceramic coatings technology in various industrial fields. The book includes topics related to the applications of ceramic coating covers in engineering, including fabrication route (electrophoretic deposition and physical deposition) and applications in turbine parts, internal combustion engine, pigment, foundry, etc.

How to reference

In order to correctly reference this scholarly work, feel free to copy and paste the following:

George E. Stan and José M.F. Ferreira (2012). Magnetron Sputtered BG Thin Films: An Alternative Biofunctionalization Approach – Peculiarities of Bioglass Sputtering and Bioactivity Behaviour, Ceramic Coatings - Applications in Engineering, Prof. Feng Shi (Ed.), ISBN: 978-953-51-0083-6, InTech, Available from: <http://www.intechopen.com/books/ceramic-coatings-applications-in-engineering/magnetron-sputtered-bg-thin-films-an-alternative-biofunctionalization-approach-peculiarities-of-biog>

INTECH
open science | open minds

InTech Europe

University Campus STeP Ri
Slavka Krautzeka 83/A
51000 Rijeka, Croatia
Phone: +385 (51) 770 447
Fax: +385 (51) 686 166
www.intechopen.com

InTech China

Unit 405, Office Block, Hotel Equatorial Shanghai
No.65, Yan An Road (West), Shanghai, 200040, China
中国上海市延安西路65号上海国际贵都大饭店办公楼405单元
Phone: +86-21-62489820
Fax: +86-21-62489821

© 2012 The Author(s). Licensee IntechOpen. This is an open access article distributed under the terms of the [Creative Commons Attribution 3.0 License](#), which permits unrestricted use, distribution, and reproduction in any medium, provided the original work is properly cited.

IntechOpen

IntechOpen